JOURNAL OF MATERIALS SCIENCE 29 (1994) 3451–3457

$FeCl_3$-doped polyvinylidene fluoride

Part I *Interpolaron hopping and optical properties*

A. TAWANSI, H. I. ABDEL-KADER, M. EL-ZALABANY*, E. M. ABDEL-RAZEK
Department of Physics, Faculty of Science, Mansoura University, 35516, Egypt
**Department of Electrical Engineering, Faculty of Engineering, Mansoura University, 35516, Egypt*

Infrared (350–4000 cm^{-1}) and optical ($1.15 \times 10^4 - 2.95 \times 10^4$ cm^{-1}) spectra, differential thermal analysis (DTA) and d.c. electrical resistivity of $FeCl_3$- doped polyvinylidene fluoride (PVDF) films, over the doping mass fraction range $0 \leqslant w \leqslant 0.40$, have been measured. The i.r. spectra provided evidence of: (a) the presence of both α and γ phases in the undoped, and a γ phase in the doped PVDF films; (b) a head-to-head content of 20%; and (c) a different doping mode beyond a 0.25 doping level. The optical spectra resulted in two induced energy bands, and a probable interband electronic transition, due to doping. Dipole relaxation and premelting endothermic peaks were identified by DTA. Electrical conduction is thought to proceed by interpolaron hopping among the polaron and bipolaron states induced by doping. The hopping distance, R_0, is calculated according to the Kuivalainen model. A numerical equation is adopted to formulate the dependence of R_0 on doping level and temperature. It is found that $R_0 <$ CC separation length. This implies that, in doped PVDF, charge carrier hopping is not an intrachain process.

1. Introduction

Since the discovery of polyvinylidene fluoride as a polymer electret [1, 2] much effort has been devoted to the better understanding of the nature of permanent polarization [3, 4], and how it gives rise to piezoelectricity [5] and pyroelectricity [6]. PVDF crystallizes into several crystal forms, namely α, β, γ [7], the planar zigzag, 2_1 helix of the β phase and the 3_1 helical structure [8]. PVDF and related semicrystalline polymers are receiving increasing attention, as these polymers find use in wide applications.

The present work is part of a systematic study of the effect of transition metal halide doping on the physical and structural properties of PVDF and their possible applications. The present work is devoted to an investigation of the effect of $FeCl_3$ doping on i.r. and optical spectra, and on the electrical conduction of PVDF films. The effect of $FeCl_3$ doping on magnetic susceptibility and on the microwave response of PVDF is investigated by Tawansi *et al.* [9].

2. Experimental procedure

Samples were made from PVDF resin provided by Solvey (Belgium) and referenced as SOLEF 1008. Dimethylformamide was used as a solvent for the resin and $FeCl_3$ dopant. Films were prepared by casting the desired solution onto glass, such that the films were approximately 0.2–0.5 mm thick after the solvent was removed at 343 K. An infrared spectrometer (Perkin Elmer 1430) was used for measuring the i.r. spectra in the wave number range, of 350–4000 cm^{-1}. A Perkin Elmer (1800) spectrometer was used for measuring optical transmittance in the wave number range of $1.15 \times 10^4 - 2.95 \times 10^4$ cm^{-1}. A thermoanalyser (GDTD 16, setaram), with a measuring temperature range of 10–200 °C, a heating rate of 2 °C min^{-1} and sensitivity 2.5 μV, was used for differential thermal analysis. Electrical resistivity was measured by a standard technique [10] using an autorange multimeter (Philips 175) of accuracy ± 0.2%. The films were in the form of circular discs, of 1.6 ± 0.001 cm diameter. Contacts were of highly conductive silver paste, with an area of 1 cm^2. A guard ring was used. The sample was short-circuited for about two days, at a constant temperature of 300 K, before the d.c. voltage was applied. Resistivity was measured in the steady-state to avoid errors due to relaxation phenomena.

3. Results and discussion

3.1. Infrared analysis

The infrared spectra (4000–350 cm^{-1}) of the undoped and 5, 15, 25, 30 and 40 wt %) $FeCl_3$ doped PVDF samples are shown in Fig. 1, and the frequency values of the observed absorption bands (compared with the bands characterizing the α and γ phases [7]) are listed in Table I. Both of the main bands of the α and γ phases are noticed in the spectrum of the undoped sample. On the other hand, the spectra of the doped samples revealed the presence of a single γ phase, and the disappearance of the α phase. The absorption bands, which are clearly influenced by doping, will be discussed as follows.

The band at 1750 cm^{-1}, which is assigned to C=C

0022–2461

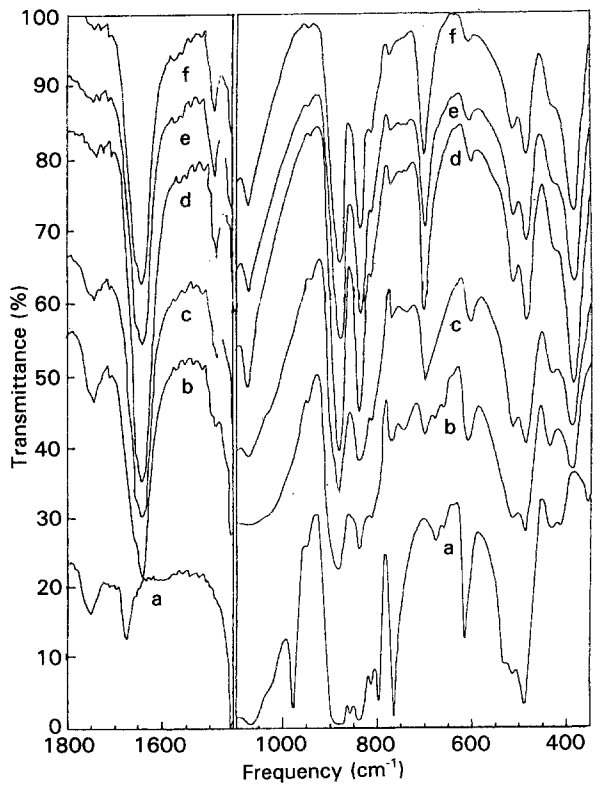

Figure 1 Infra red spectra of (a) undoped, (b) 5, (c) 15, (d) 25, (e) 30 and (f) 40 wt % $FeCl_3$ doped PVDF.

stretching in the difluorinated alkenes

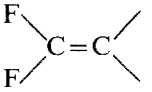

is weakened by doping. The band at 1675 cm^{-1}, which is assigned to C=C stretching [11] in the trans-disubstituted ethylene

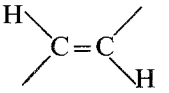

exhibited a medium relative intensity in the case of the undoped samples, and it is transformed to a shoulder by doping. This shoulder form may be due to overlap with the nearest neighbouring strong band at 1642 cm^{-1}, for the doped samples. The band at 1642 cm^{-1}, is assigned to the C=C stretching in the monofluorinated alkenes

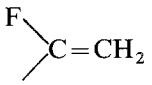

The band at 1488 cm^{-1}, appeared for the doped samples only, is assigned to CH_2 bending mode at the head-to-head (h-to-h) units [12].

TABLE I Frequency values of observed i.r. absorption bands compared with those characterising the α and β phases.

Phase		$FeCl_3$ (wt %)					
α	γ	0	5	15	25	30	40
3029	3026	3030	3030	3030	3030	3020	3020
2989	2984	2990	2984	2984	2984	2980	2980
–	–	1750	1750	1750	1750	1750	1750
–	–	1675	1675 (sh)	1675 (sh)	1675 (sh)	1675 (sh)	1675 (sh)
–	–	–	1642	1642	1642	1642	1642
–	–	–	1488	1488	1488	1488	1488
–	1454	1454	1454	1454 (sh)	1454 (sh)	1454 (sh)	1454 (sh)
–	1412	–	1415	1415	1410	1410	1410
1399	–	1400	–	–	–	–	–
–	1335	1335	1335	1335	1340	1335	1335
–	1075	1075	1075	1075	1078	1075	1075
1067	–	1065	–	–	–	–	–
976	–	976	–	–	–	–	–
–	950	950	950	948	948	948	945
–	880	880	880	880	880	880	880
856	–	856	–	–	–	–	–
–	840	838	840	840	840	840	840
–	812	812	815	815	815	815	815
796	–	796	–	–	–	–	–
–	–	–	775	775	775	773	773
765	–	765	–	–	–	–	–
–	–	–	700	700	702	700	700
–	–	676	–	–	–	–	–
–	–	660	–	–	–	–	–
616	–	616	–	–	–	–	–
612	613	613 (sh)	–	–	–	–	–
–	–	610 (sh)	609	605	605	602	602
531	–	530	–	–	–	–	–
–	512	512	–	–	–	–	–
489	–	490	–	–	–	–	–
–	482	–	482	482	482	482	482
–	430	430	433	430	425	425	425
–	–	–	385	385	385	385	385
355	–	354	–	–	–	–	–

The bands at 880, 840, 700 and 385 cm^{-1}, exhibit maximum relative intensity values at 25 wt % $FeCl_3$ doping. The band at 880 cm^{-1}, is assigned to symmetric stretching of CF_2 and to out-of-phase symmetric stretching of CC. The band at 840 cm^{-1}, is assigned to stretching of CH_2 and to out-of-phase antisymmetric stretching of CF_2. The band at 700 cm^{-1}, is assigned to the CF_2 wagging mode of the h-to-h, CF_2CF_2, units. Kobayashi *et al.* [7] found that the frequency of this mode is strongly dependent upon the amount of h-to-h content.

In the present i.r. spectra, the band at 700 cm^{-1} indicates a h-to-h content of 20%. The band at 385 cm^{-1}, is assigned to the CF_2 bending mode.

It is noteworthy that the potential energy distribution [7] along the PVDF chain is strongly affected by structural disorder [13], monofluorinated segments [14], polar group substituted ethylene [15] and h-to-h and tail-to-tail units. This may be evidence for local deformation due to polaron and bipolaron defects [16].

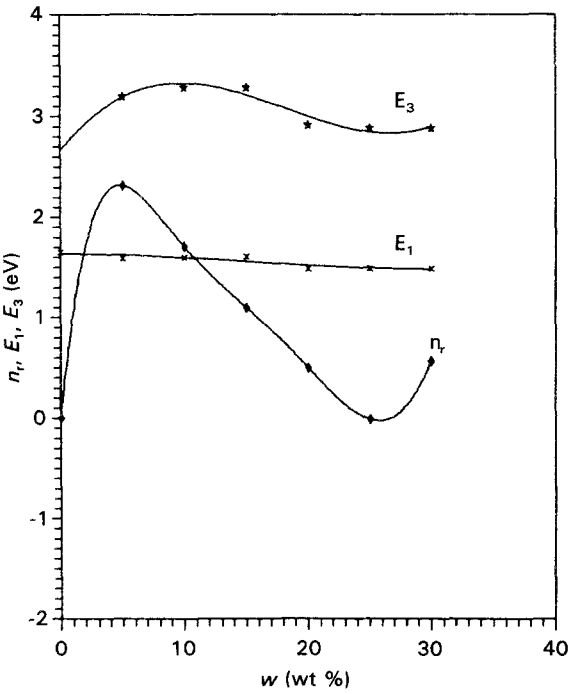

Figure 3 The doping level dependence of E_1, E_3 and n_r.

3.2. Optical transmittance

Optical transmission spectra for undoped, 5, 10, 15, 20, 25, and 30 wt % $FeCl_3$ doped PVDF, are shown in Fig. 2a,b. A clear absorption band is observed, typically at 1.33×10^4 cm^{-1} for undoped PVDF, indicating the presence of an induced shallow energy band, of depth, E_1 (= 1.65 eV), below the conduction band, and indicating an interband electronic transition. The increase in $FeCl_3$ doping revealed a slight decrease in E_1, as shown in Fig. 3. If t_1 and t_2 represent the transmittance at E_1 and the maximum transmittance of the spectrum, respectively, then $\Delta t = (t_2 - t_1)$ may be taken as a measure of the density of the electrons in the induced band. Let $\Delta t_0 = t_2 - t_1$ for the undoped PVDF. Thus, the relative change in the density of induced electrons due to doping is

$$n_r = (\Delta t - \Delta t_0)/\Delta t_0 \quad (1)$$

The calculated values of n_r are plotted as a function of the doping level, w, in Fig. 3. A peak and a minimum are noticed for n_r at doping levels of 5 and 25 wt %, respectively. Accordingly, the change in n_r due to doping can be classified into three (low, moderate and high) regions. Each region is characterized by a certain mode of doping.

A relatively deep absorption band is observed in Fig. 2, for the spectra of the doped PVDF, indicating another doping induced energy band, of E_3 edge

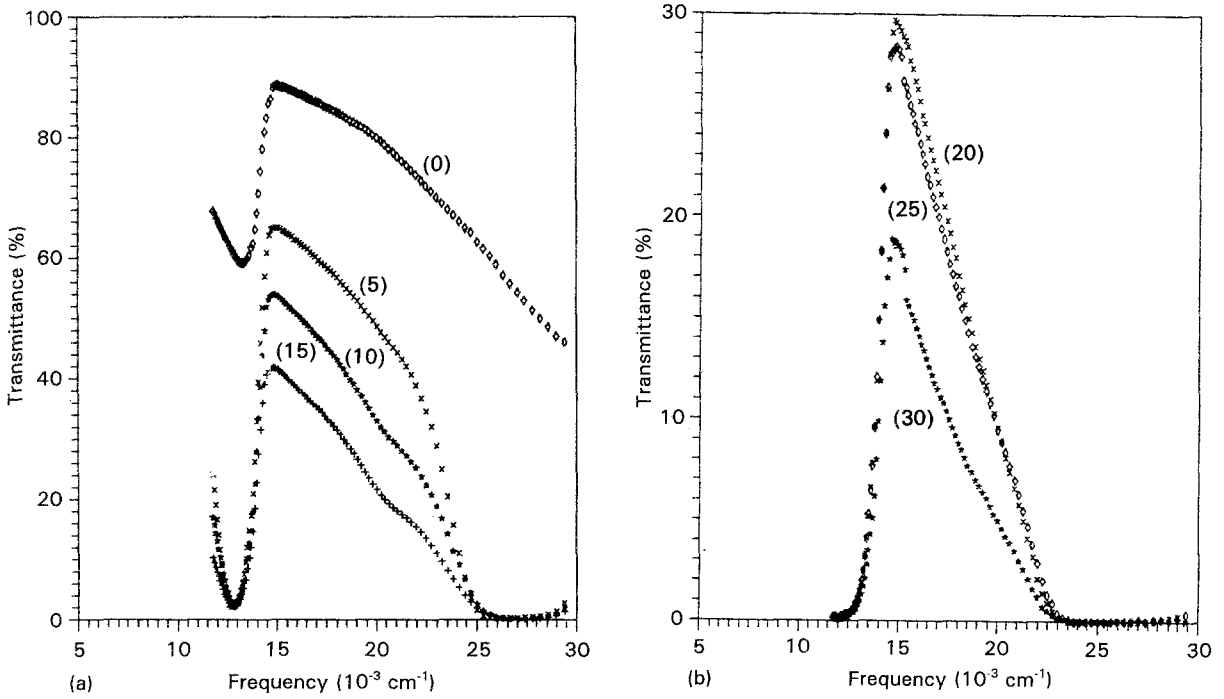

Figure 2 Optical transmission spectra of: a) undoped, 5, 10 and 15 wt % $FeCl_3$ doped PVDF: b) 20, 25 and 30 wt % $FeCl_3$ doped PVDF.

depth, below the conduction band. The calculated E_3 values for various dopant levels are shown in Fig. 3. It is remarkable that w affects E_3 more predominantly than E_1. Broad maximum and minimum of E_3 are observed at 10 and 25 wt % doping levels, respectively.

3.3. Differential thermal analysis

The comparative DTA diagrams of 5 and 35 wt % $FeCl_3$ doped PVDF samples are presented, on an arbitrary scale, in Fig. 4. Clear endothermic peaks are noticed at 179 and 170 °C for 5 and 35 wt % doping levels, respectively. These peaks can be attributed to premelting temperatures [17]. A broad endothermic peak is observed at 47 °C, for the 35 wt % doping level. This peak is thought to have arised from dipole relaxation due to molecular motion of the doping halide [18, 19].

3.4. D.c. electric conduction

D.c. electrical resistivity, ρ, was measured in the temperature, T, range of 353–433 K for the PVDF films doped with 5, 10, 15, 20, 25, 30, 35 and 40 wt % $FeCl_3$. Arrhenius plots of the resistivity are shown in Fig. 5a,b. The linear regions of these plots obey Arrhenius equation

$$\rho = \rho_0 \exp(E/kT), \quad (2)$$

where ρ_0 is a pre-exponential factor, E is the activation energy and k is the Boltzmann constant. It is noticed that for doping levels $\geqslant$ 20 wt % the Arrhenius relation could be applied in a limited temperature range. The calculated values of E for various doping levels, using Equation 2, and the linear plots of Fig. 5a,b, are shown in Fig. 6. The value of E increases, expo-

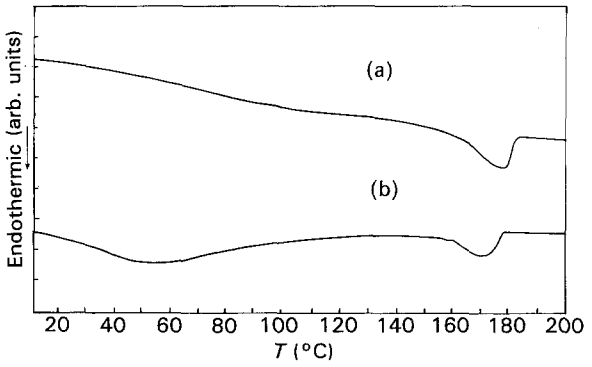

Figure 4 Comparative DTA diagrams of: (a) 5 and (b) 35 wt % $FeCl_3$ doped PVDF.

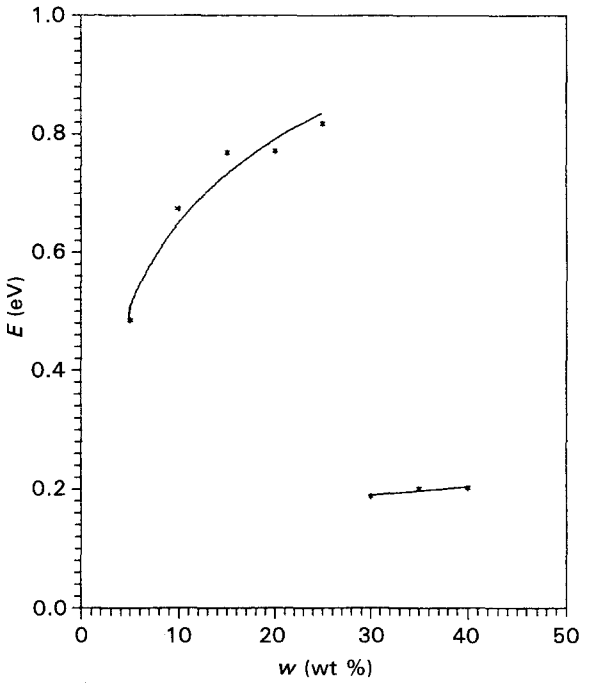

Figure 6 Doping level dependence of activation energy, E.

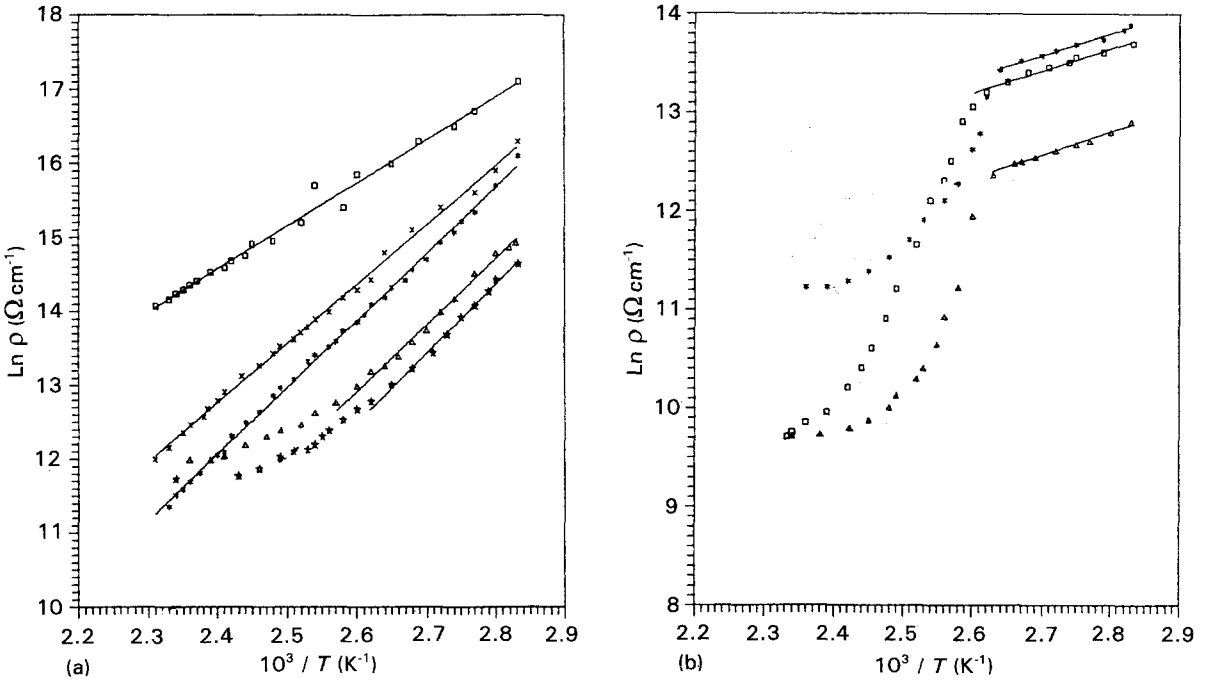

Figure 5 Arrhenius plots of ρ for: a) (□) 5, (×) 10, (*) 15, (△) 20, (☆) 25: b) (*) 30, (□) 35, (△) 40 wt % $FeCl_3$ doped PVDF.

nentially (from 0.4 to 0.8 eV) as w increases from 5 to 25 wt %. For $w \geqslant 30$ wt % the value of E decreases steeply to $\simeq 0.2$ eV.

Das-Gupta *et al.* [3] studied the electric conduction of undoped PVDF, in the temperature range of 293–413 K, and found that ionic conduction proceeds in PVDF where the carriers hop through the defect sites along the polymeric chains, according to a model previously proposed by Mott and Gurney [20]. Das-Gupta *et al.* [3] found that the average jump distance of the charge carrier is $\simeq 2.5$ nm (of $\simeq 10$ monomer units, knowing that the PVDF monomer unit has a length of $\simeq 0.25$ nm [20]). The obtained jump distance equals the separation of two successive h-to-h defects, assuming $a \sim 50\%$ crystallinity and $a \sim 10\%$ h-to-h defect, which lies mainly in the amorphous phase. Thus the h-to-h defects are considered as jumping sites for the charge carriers.

The Mott and Gurney hopping model [20] resulted in unreasonable parameters for the $FeCl_3$ doped PVDF samples in the present work, and has hence been ruled out. Moreover, the $T^{-1/4}$ and $T^{-1/2}$, resistivity dependences, variable range hopping models [21, 22] also revealed unexpected values for the hopping energy and density of states near the Fermi level for the present samples.

Kivelson [23, 24] proposed a conduction model based on phonon-assisted hopping between soliton bound states in lightly doped polyacetylene. This intersoliton hopping is a three-dimensional conduction between a neutral and a charged soliton in the vicinity of dopants. Later Kuivalainen *et al.* [16] slightly modified Kivelson's model and applied it to quasi one-dimensional conduction processes between polaron and bipolaron states in polyparaphenylene. Since the distribution of the site energies is narrow, the hopping processes in this model are isoenergetic. According to Kuivalainen *et al.* [16] resistivity due to interpolaron hopping is expressed as

$$\rho = kT/Ae^2\gamma(T)(R_o^2/\xi) \times [(Y_p + Y_{bp})^2/(Y_p Y_{bp})]\exp(2BR_o/\xi) \quad (3)$$

where $A = 0.45$; $B = 1.39$; Y_p, Y_{bp} are the concentration of polarons and bipolarons respectively; and $R_o = (3/4\pi C_{imp})^{1/3}$ is the typical separation between impurities whose concentration is C_{imp}. $\xi = (\xi_{||}\xi_{\perp}^2)^{1/3}$ is the average decay length of a polaron or bipolaron wave function, and $\xi_{||}$ and $\xi_{\perp}$ are the decay length parallel and perpendicular to the polymer chain, respectively. According to the calculation of Bredas *et al.* [25] the extension of the defect should be the same for polarons and bipolarons. The transition rate of an electron between polaron and bipolaron states can be expressed as

$$\gamma(T) = \gamma_o(T/300k)^{n+1} \quad (4)$$

where n is constant, ~ 10, and the prefactor, γ_o, equals $1.2 \times 10^{17}\ s^{-1}$ was estimated by Kivelson [23].

In the present work, the order of magnitude of ρ was adjusted with the impurity concentration, C_{imp}, which actually was the fitting parameter. The parameter $\xi_{||}$ equals 1.06 nm, while the value of $\xi_{\perp}$, which depends on the interchain resonance energy and the interchain distance, $b = 0.452$ nm [8], is not known for PVDF and was estimated from the relation [26] $\xi_{\perp} = b/2$. Taking $Y_p = Y_{bp}$ for simplicity, which is a reasonable approximation, and using Equations 3 and 4 one can obtain the values of the separation between impurities, R_o.

Fig. 7 depicts the $\ln\rho$ versus $\ln T$ plots for variously $FeCl_3$ doped PVDF samples. The linear parts of these plots correspond to the temperature ranges in which the interpolaron hopping proceeds. Fig. 8 shows the doping level dependence of R_o, calculated at $T = 353$ K, which can be expressed as

$$R_o = (1.618)\exp(-0.048)w \quad (5)$$

It is remarkable that $R_o \leqslant 0.13$ nm, which is less than

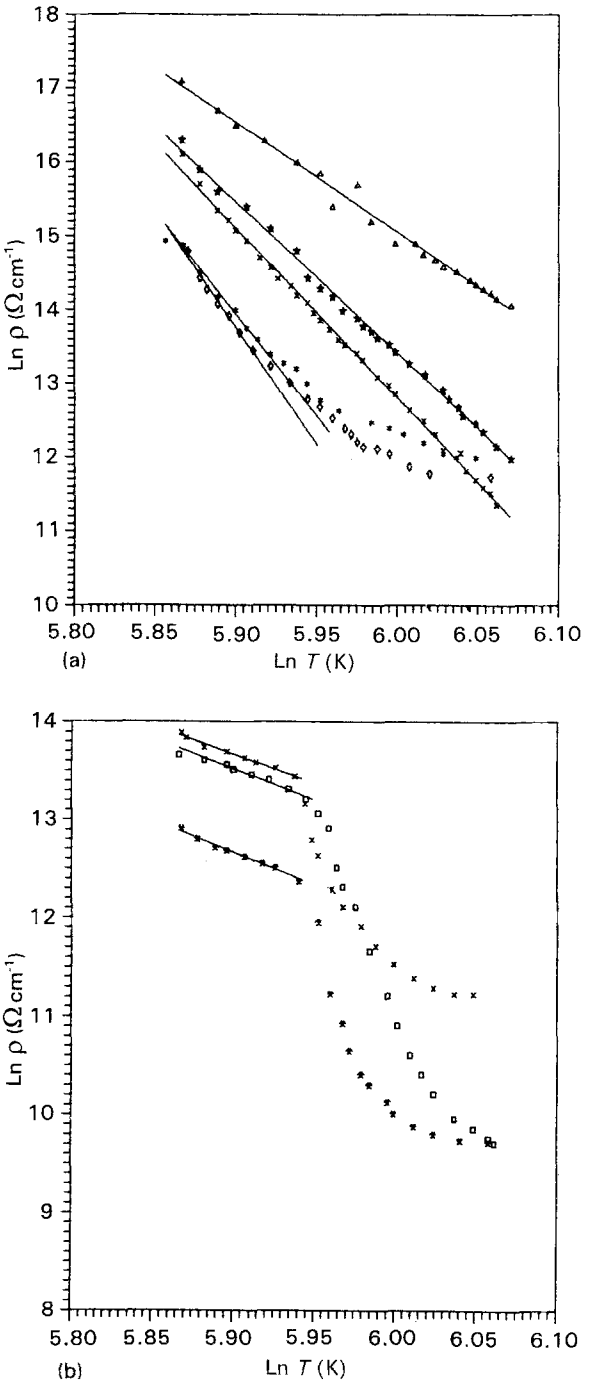

Figure 7 Ln ρ against ln T plots for: a) (△) 5, (☆) 10, (×) 15, (*) 20, (◇) 25: b) (×) 30, (□) 35, (*) 40 wt % $FeCl_3$ doped PFDV.

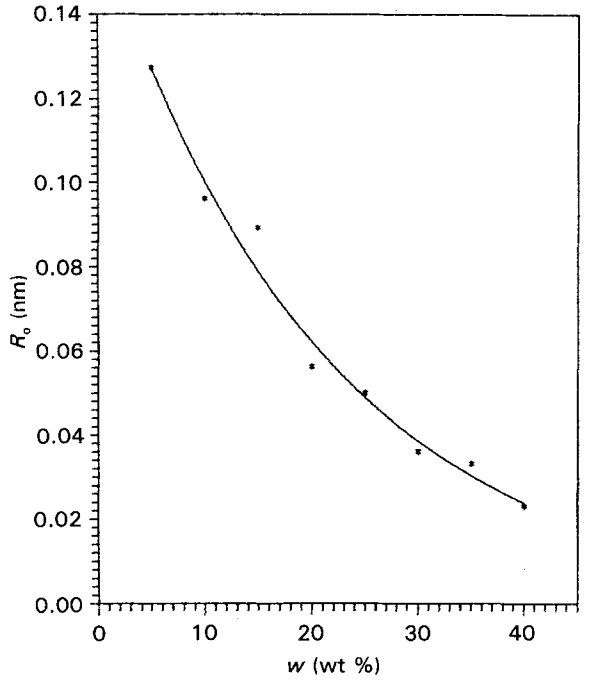

Figure 8 Doping level dependence of R_0 calculated at $T = 353$ K.

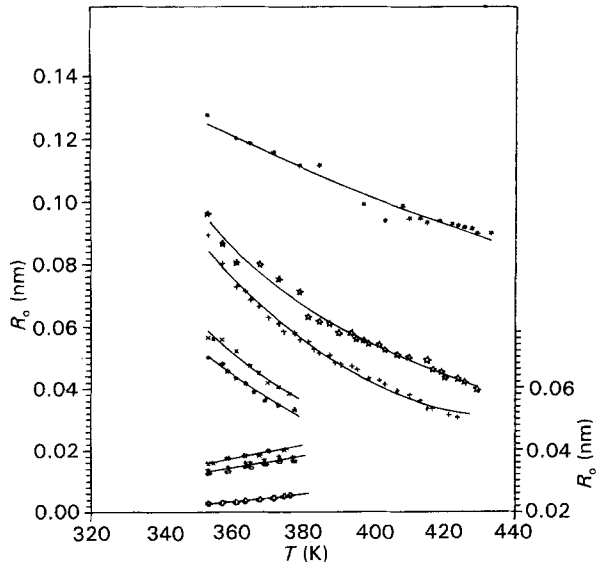

Figure 9 Temperature dependence of R_0 for various $FeCl_3$ doping levels in PVDF.

the separation between two successive h-to-h sites (~ 1.25 nm of 5 monomer units, corresponding to 20% h-to-h content, implied from i.r. analysis). R_0 is even less than the monomer unit length (~ 0.25 nm [20]). Thus, it is believed that there are additional hopping sites formed by dopant molecules. Fig. 9 depicts the temperature dependence of the hopping distance, for various doping levels, which obeys the formula

$$R_0 = L\exp(25 - w + MT) \quad (6)$$

where the values of the two parameters L and M are listed in Table II.

It is noticed that for doping levels $\leqslant 25$ wt %, R_0 decays exponentially as T increases. This may be

TABLE II Doping level dependence of L and M parameters.

w (wt %)	L	M
5	1.246×10^{-8}	− 0.0045
10	1.261×10^{-5}	− 0.0108
15	5.552×10^{-3}	− 0.0142
20	2.41	− 0.0182
25	348.105	− 0.0185
30	798.5	0.0054
35	1134.36	0.0053
40	148 413.39	0.0046

evidence for the role of thermally induced hopping sites, due to liberation of new charge carriers. On the other hand, for doping levels $\geqslant 30$ wt % a slight exponential increase of the hopping distance is observed as T increases. This apparent increase in R_0 is thought to be due to probable back and forth hopping effects that include a generalized dwelling time [27]. The dwelling time is defined as [28] the mean time a carrier stays at a certain site, including the possibility of leaving the site and returning. This is an acceptable argument, because for such disordered systems the hopping transport [29] is believed to be a trap-limited process in which a low density of localized sites (traps) is energetically separated from a higher density main hopping channel [30]. Carriers hopping into such traps require extra energy to hop back onto the main transport channel [31].

It could be concluded that the polaron, bipolaron and induced energy states due to doping act as hopping sites for the charge carriers. Accordingly, for the $FeCl_3$ doped PVDF, the conduction process is not of an intrachain type, i.e. it is not an ideal one-dimensional mechanism.

References

1. H. KAWAI, *Jpn. J. Phys.* **8** (1969) 975.
2. A. M. GLASS, J. H. McREE and J. G. BERGMAN Jr, *J. Appl. Phys.* **42** (1971) 5219.
3. D. K. DAS-GUPTA, K. DOUGHTY and R. S. BROCKLEY, *J. Phys. D: Appl. Phys.* **13** (1980) 2101.
4. R. M. FARIA, J. S. NOGUEIRA and N. ALVES, *ibid.* **25** (1992) 1518.
5. J. E. McKINNER, G. T. DAVIS and M. G. BROADHURST, *J. Appl. Phys.* **51** (1980) 1676.
6. F. I. MOPSIK and A. S. DE REGGI, *Appl. Phys. Lett.* **44** (1984) 65.
7. M. KOBAYASHI, K. TASHIRO and H. TADOKORO, *Macromolecules* **8** (1975) 158.
8. R. ZHANG and P. L. TAYLOR, *J. Chem. Phys.* **94** (1991) 3207.
9. A. TAWANSI, H. I. ABDEL-KADER, W. BALACHANDRAN and E. M. ABDEL-RAZEK, *J. Mater. Sci.* in press.
10. A. TAWANSI, N. KINAWY and M. EL-MITWALLY, *ibid.* **24** (1989) 2497.
11. I. FLEMING and D. H. WILLIAMS, "Spectroscopic Methods in Organic Chemistry" (McGraw-Hill, New York, 1966) pp. 56.
12. G. ZERBI, *Pure & Appl. Chem.* **26** (1971) 499.
13. M. A. BACHMANN, W. L. GORDON and J. B. LANDO, *J. Appl. Phys.* **50** (1979) 6106.
14. R. HASEGAWA, M. KOBAYASHI and H. TADOKORO, *Polym. J.* **3** (1972) 591.
15. R. C. NEWMAN, "Infrared Studies of Crystal Defects" (Taylor and Francis, London, 1973) pp. 89.

16. P. KUIVALAINEN, H. STUBB, H. ISOTLO, P. YLI and C. HOLMSTROM, *Phys. Rev. B* **31** (1985) 7900.
17. S. ELIASSON, *J. Phys. D: Appl. Phys.* **18** (1985) 275.
18. P. C. MEHENDRA, S. CBAND, *ibid.* **16** (1983) 185.
19. M. LATOUR, K. ANIS and R. M. FARIA, *ibid.* **22** (1989) 806.
20. N. F. MOTT and R. W. GURNEY, "Electronic Processes in Ionic Crystals" (OUP, London, 1940) pp. 34.
21. K. C. KAO, *J. Phys. D: Appl. Phys.* 17 (1984) 1433.
22. A. L. EFROS and B. I. SHKLOVSKII, *J. Phys. C* **8** (1979) 149.
23. S. KIVELSON, *Phys. Rev. B* **25** (1982) 3798.
24. *Idem., Mol. Cryst. Liq. Cryst.* **77** (1981) 65.
25. J. L. BREDAS, R. R. CHANCE and R. SILBEY, *Phys. Rev. B* **26** (1982) 5843.
26. S. KIVELSON, *Phys. Rev. Lett.* **46** (1981) 1344.
27. A. TAWANSI, S. EL-KONSOL, A. F. BASHA and M. M. MORSI, *Acta Physica Hungarica* **54**(3–4) (1983) 221.
28. B. MOVAGHAR, B. POHLMANN and W. SCHIMACHER, *Phil. Mag. B* **41** (1980) 49.
29. A. TAWANSI, M. D. MIGAHED and M. I. A. EL-HAMID, *J. Phys. D: Appl. Phys.* **20** (1987) 772.
30. G. PFISTER and H. SCHER, *Adv. Phys.* **27** (1978) 747.
31. G. PFISTER and M. MORGAN, *Phil. Mag. B* **41** (1980) 191.

Received 11 May
and accepted 10 December 1993